Chloroperoxidase, a Janus Enzyme[†]

Kelath Murali Manoj*[,‡] and Lowell P. Hager*

Department of Biochemistry, University of Illinois at Urbana–Champaign, 6000 South Mathews Avenue, Urbana, Illinois 61801

Received November 13, 2007; Revised Manuscript Received December 28, 2007

ABSTRACT: Chloroperoxidase is a versatile fungal heme-thiolate protein that catalyzes a variety of one-electron and two-electron oxidations. We report here that the alkylation of an essential histidine residue showed no effect on the one-electron peroxidations but inhibited two-electron oxidations. The pH profiles of different peroxidative substrates showed optimal activities at varying pH values for the same enzyme. 2-Allylphenol and substituted *ortho*-phenolics showed efficient peroxidations. Also, substrates excluded from the active site (or with no favorable positioning at the heme center or heme edge) were converted in the peroxidation reaction. While hydrogen peroxide serves as the superior activator in the two-electron oxidations, small alkylhydroperoxides give much better rates for peroxidation reactions. All the above observations indicate that one-electron oxidations are mechanistically quite different from the two-electron oxidations catalyzed by chloroperoxidase. We propose that the peroxidatic substrates interact predominantly outside the heme active site, presumably at the surface of the enzyme.

Recent studies have indicated that chloroperoxidase (CPO),[1] a glycosylated hemoprotein secreted by the fungus *Caldariomyces fumago*, is an enzyme of ecological and social significance (*1, 2*). Since the discovery of this enzyme in the early 1960s (*3*), several facets of its catalytic activity have surfaced (*4*). After the activation of ferric heme center by a suitable hydroperoxide, CPO carries out a wide variety of oxidative reactions. In the early years, the focus was on its signature halogenation reactions (*5–7*). Later, the enantioselective oxygen insertion reactions generated much interest (*8–10*). The latter reactions hold high industrial potential for generating chiral synthons (*4*). Like a true peroxidase, CPO also catalyzes the reactions of single electron or hydrogen atom abstractions (or peroxidations) from electron-rich molecules. In early studies, CPO exhibited relatively lower ability in peroxidatic reactions when compared with analog enzymes like horseradish peroxidase (*11, 12*). Perhaps owing to this fact, fewer publications have dealt with this facet of CPO's catalytic repertoire.

In our continuing efforts to elucidate the functions of this highly versatile enzyme, we have investigated single-electron peroxidations catalyzed by CPO. It has been established that the two-electron processes of oxygen insertion or peroxide dismutation reactions occur within the heme active site (*13*) and the chlorination reaction is mediated via a diffusible species (*14*). Here, we report observations that indicate that the peroxidative substrates interact with CPO via yet another mode, presumably at the surface of the enzyme. Unlike most enzymes, which usually have one well-defined active site catalyzing a specific reaction, CPO exhibits multiple interactive mechanisms with its diverse substrates. This is quite analogous to the mythical Roman god Janus (god of doors, gates, and passageways), who is portrayed with multiple faces.

MATERIALS AND METHODS

Commercially available *N*,*N*,*N*′,*N*′-tetramethylphenylene diamine (TMPD, free base), 2,2′-azino-bis(3-ethylbenzothiazoline-6-sulfonic acid) (ABTS, diammonium salt), pyrogallol,and guaiacol were employed as substrates. Oxidation reactions were not studied above pH 7 because in these ranges, CPO undergoes a structural alteration to give a functionally inactive enzyme (*15*).

General Methods. Reactions of 1–3 mL volumes were carried out in plastic, glass,or quartz cuvettes at room temperature (20–22 °C). The reaction was initiated by adding a suitable amount of appropriately diluted enzyme or hydroperoxide. The initial rate of change of absorbance or the optical density measured after a given time (using Shimadzu UV–vis 2401PC spectrophotometer) was used for the calculation of initial rates or conversion (respectively), using the extinction coefficient of products at the designated wavelength. The molar extinction coefficients (per centimeter) were 3.6×10^4 at 414 nm for the ABTS radical cation (*16*), 1.247×10^4 at 563 nm for the TMPD radical cation (*17*), and 2.64×10^3 at 420 nm for purpurogallin (*18*). It should be noted that though guaiacol is a commonly used phenolic peroxidative substrate, many aspects of its assay still remain unresolved. Maehly and Chance (*19*) had first proposed that its oxidative product was an oligomer, tetraguaiacol. However, in 1997, Doerge et al. established the

[†] This work was financed by NIH Grant RG7768 and Satyamjayatu.

* Corresponding authors. For K.M.M.: phone, +91-9995089671; fax, +91-480-2897337; e-mail, satyamjayatu@yahoo.com. For L.P.H.: phone, 217-333-9686; fax, 217-244-5858; e-mail, l-hager@uiuc.edu.

[‡] Current address: Biotechnology Department, MET's School of Engineering, Mala, Kuruvilassery (PO), Thrissur District, Kerala State 680735, India.

[1] Abbreviations: ABTS, 2,2′-azino-bis(3-ethylbenzothiazoline-6-sulfonic acid); CPO, chloroperoxidase; DBTD, 3,3′-dimethoxy-bicyclohexylidene-2,5,2′,5′-tetraene-4,4′-dione; DEPC, diethyl pyrocarbonate; DMPC, dimethyl pyrocarbonate; EtOOH, ethyl hydroperoxide; MCD, monochlorodimedone; TBPD, *N*,*N*,*N*′,*N*′-tetrabenzylphenylene diamine; TMPD, *N*,*N*,*N*′,*N*′-tetramethylphenylene diamine.

10.1021/bi7022656 CCC: $40.75
Published on Web 01/26/2008

Table 1: The Percentage Residual Activities after Various Time Periods of Incubation of CPO with Dimethyl and Diethyl Pyrocarbonates[a]

							peroxidation			
	dismutation		chlorination		epoxidation		ABTS		TMPD	
time (min)	DMPC	DEPC	DMPC	DEPC	DMPC	DEPC	DMPC	DEPC	DMPC	DEPC
0	100	100	100	100	100	100	100	100	100	100
10	59	56	58	59	67	52	80	87	94	98
30	38	44	36	38	43	44	73	81	83	102

[a] Please refer to the Materials and Methods section for details.

Scheme 1: Mass and Charge Balanced Equations of Peroxidative Reactions in Current Study

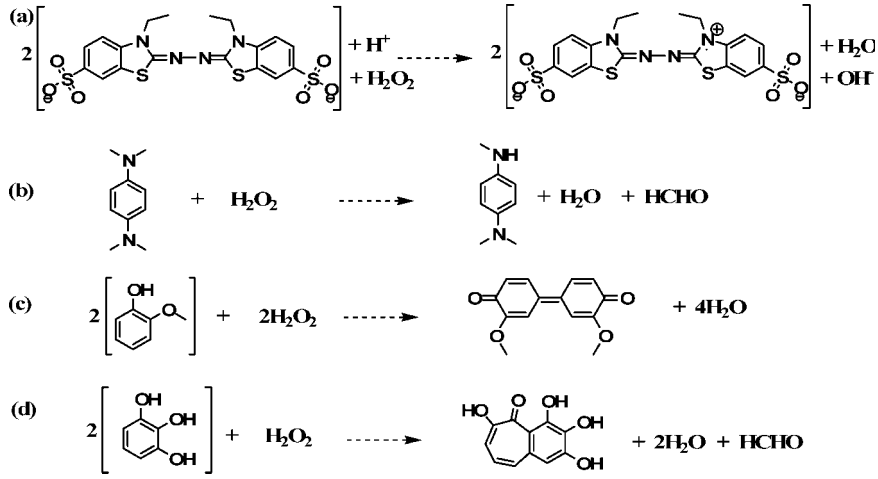

true identity of the chromophore as 3,3′-dimethoxy-bicyclohexylidene-2,5,2′,5′-tetraene-4,4′-dione (or DBTD, also cited as 3,3′-dimethoxy-4,4′-biphenylquinone) (*20*). Such a reaction calls for a multielectron oxidation mechanism, most probably involving complex radical chemistry. The initiative first-electron process is understood to be from the enzyme, but the origin of the latter ones is not yet established. Regardless, several researchers continue to cite the product as "tetraguaiacol" or "guaiacol oligomer". Since researchers from diverse fields have continued to use the ϵ value of 2.66 $\times$ 10^4 M^{-1} cm^{-1} for the product at 470 nm, we adopt the same for relative comparison of data.

Dimethyl and Diethyl Pyrocarbonate (DMPC and DEPC) Derivatization and Specific Enzyme Assays for Table 1. The 1 mL reaction mixture contained 940 μL of pH 6.5 buffer (100 mM potassium phosphate), 40 μL of 65 mg/mL CPO, and 20 μL of 300 mM DMPC or DEPC solution in acetonitrile. The pyrocarbonate solution was added to start the deactivation reaction. The reaction mixture was incubated at 20–22 °C. The positive control reaction was also subjected to the same procedure but contained 20 μL of acetonitrile lacking the dialkylpyrocarbonates. After the specified incubation intervals, 167 μL samples were withdrawn and diluted with 300 μL of pH 4.0 phosphate buffer and rapidly centrifuged at 14 000 rpm in Eppendorf tubes fitted with a YM30 filter. The treated enzyme was recovered and washed three times with excess buffer. All recovered samples were then made up to a final volume of 500 μL. Suitable aliquots of this recovered enzyme solution were taken for the five different assays. A negative control of bovine serum albumin with DMPC or DEPC subjected to the same procedure did not give any significant reaction in any of the five assays. In the reaction assays conducted below, increasing amounts of enzyme from 0 to 100% gave a corresponding linear increase in activity. The values reported in the table are relative to the positive control. The five assays were conducted as follows.

Hydroperoxide Dismutation. The reaction was monitored at 240 nm. The reaction mixture contained 40 μL of 880 mM H_2O_2, 960 μL of pH 4 buffer, and 10 μL of the pyrocarbonate-treated enzyme.

MCD Chlorination. The reaction was monitored at 278 nm. The standard 3 mL reaction conditions were used (*5*) with 10 μL of a 10-fold diluted aliquot of the treated enzyme.

Indene Epoxidation. The reaction was monitored at 250 nm (*21*). The reaction mixture had 965 μL of pH 5.0 buffer, 17 μL of 120 mM H_2O_2, 20 μL of 8 mM indene in acetonitrile, and 10 μL of the modified chloroperoxidase.

ABTS Peroxidation. The reaction was monitored at 414 nm. The reaction mixture contained 960 μL of pH 4.0 buffer, 20 μL of 50 mM ABTS, 17 μL of 120 mM H_2O_2, and 10 μL of a 10-fold diluted aliquot of the treated enzyme.

TMPD Peroxidation. The reaction was monitored at 563 nm. The reaction mixture contained 950 μL of pH 6.5 buffer, 20 μL of 50 mM TMPD (in acetonitrile), 17 μL of 120 mM H_2O_2, and 10 μL of the treated enzyme.

Catalytic Scheme and Treatment of Data. Scheme 1 shows a charge and mass equated representation of some of the reactions studied. Though the overall order of the reactions has not yet been established clearly, the rate data are reported as a pseudo-first-order consideration (nanomolar product formed by nanomolar enzyme per second). The peroxidation reaction involves the formation of a stable radical cation centered on the nitrogen atom for the nitrogenous substrates, and the phenolic substrates give oligomerized reaction products after complex processes involving radical chemistry. Since one molecule of purpurogallin or DBTD is formed from two molecules of pyrogallol or guaiacol, respectively,

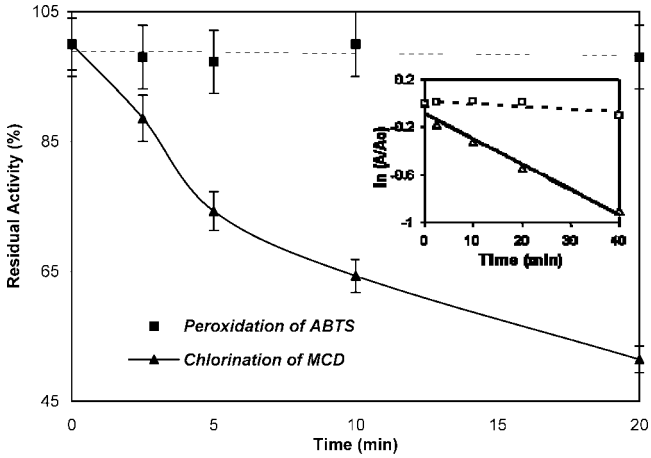

FIGURE 1: The effect of alkylation of histidine on chlorination and peroxidation reactions catalyzed by CPO. For DMPC derivatization, to 8 μL of 65 mg/mL CPO taken in 184 μL of pH 6.5 buffer, 8 μL of 1200 mM DMPC was added. The final concentration of CPO was 60 μM, and that of DMPC was 48 mM. At various intervals, 10 μL samples were withdrawn, and 490 μL of cold pH 4 buffer was added, followed by rapid centrifugation. The enzyme−DMPC reaction aliquot was made up to 500 μL, and assays for chlorination and peroxidation were carried out at pH 3 with 5–10 μL of the enzyme sample. The inset shows a logarithmic plot of remaining activity vs time of incubation with DMPC. The empty squares and triangles correspond to peroxidation and chlorination respectively.

the appropriate correction factor was used to determine the amount of substrate converted. The values of rates shown in the figures for the nitrogenous substrates are derived after subtracting the autocatalytic rates obtained in the absence of enzyme, within the first few seconds or minutes of initiation of reaction. The phenolic substrates showed no significant rates of autocatalysis in the regimes studied. Wherever error bars are not provided, it implies that the data have <15% error margins.

RESULTS

1. Effect of modification of CPO with Dialkylpyrocarbonate. Dialkylpyrocarbonate is known to affect the chlorinating activity of chloroperoxidase, most probably by the alkylation of an essential histidine (*22*). His105 is the logical candidate since it is present in the distal heme pocket, close to the Glu183 residue (*23, 24*). Table 1 shows that the covalent modification of the histidine residue also inhibits the epoxidation and peroxide dismutations catalyzed by CPO. Surprisingly, it was found that the peroxidative activities are relatively less perturbed by reaction with both dimethyl and diethyl pyrocarbonate (Table 1). Figure 1 compares the residual rates of ABTS peroxidation and MCD chlorination by CPO treated with DMPC at initial times, in a milder reaction condition. It can be seen that the peroxidation reaction is minimally perturbed by the essential histidine modification.

2. The pH Profiles of Peroxidation for Nitrogenous and Phenolic Compounds. Figure 2 shows the effect of pH for the peroxidation of various substrates. A linear correlation was derived between the concentration of hydronium ions and the enzymatic rate of peroxidation of ABTS (results not shown). CPO showed high peroxidation rates at acidic and neutral pH and lower rates in between for TMPD. In contrast to the nitrogenous compounds, relatively high variations were not seen across the pH range studied for the phenolics. The time profiles showed slightly sigmoidal traces at lower pH and hyperbolic traces at higher pH for guaiacol (results not shown). Pyrogallol peroxidation effectively occurred over a broad pH range, with a slight lowering around pH 3 and marginally enhanced activities around the acidic and neutral pH values. On the other hand, guaiacol peroxidation diminishes with increasing pH values. The reactions in the pH range of 6−7 terminated earlier than the reactions at acidic pH with both pyrogallol and guaiacol (results not shown). Pyrogallol showed several-fold higher reactivity than guaiacol. While pyrogallol showed ~30% conversion at the optimum pH, guaiacol only showed 0.75% conversion in a time of 1 min under identical conditions.

3. Peroxidation of Other Substrates of Varying Moieties and Dimensions. Earlier mechanistic hypotheses for the peroxidation reactions proposed that the substrate molecule should be positioned in close proximity to the metal center or heme edge (*25, 26*). Figure 3 shows the time course spectra of CPO catalyzed peroxidation of *ortho*-substituted cresols. The absorbance at 313 nm can be taken as an index of peroxidative reaction. Increasing the bulk of substitution in *ortho*-phenolics lowered peroxidation rates. For example, when the substitution at the *ortho* position was changed from $-CH_3$ to $-C(CH_3)_3$, the rate was found to be lowered by a factor of ~10. It is very difficult to imagine that a *tert*-butyl *ortho*-substituted phenolic can efficiently interact with the metal center or heme edge of CPO via the hydroxyl moiety. Changing the substitutions at *meta* or *para* position also gave efficient and peroxidation reactions (results not shown). These observations are contrary to the ones reported for phenolic substrates in CPO-catalyzed peroxidations (*26*). Previous studies have shown the active site mechanism based inhibition of CPO by terminal olefins (*27*). Therefore, a terminal olefin like *o*-allylphenol should generate the stable green inactive form of CPO, if the reaction occurred at the active site. However, *o*-allylphenol showed similar peroxidation rates when compared with the control molecule of *o*-propylphenol (shown in the inset of Figure 3). Other substrates like eugenol, *p*-aminostyrene, and *o*-dianisidine were also efficiently used by CPO in the peroxidation reaction at concentrations of the substrates reaching a few tens to a couple of hundreds of micromolar ranges (results not shown).

Benzylidene bis-dimethylaniline and *N*′,*N*′,*N*′,*N*′-tetrabenzyl phenylenediamine (TBPD) are molecules too big and geometrically disfavored for finding access to the heme, given the constrained active site of CPO (*14, 23, 24*). They were also reacted upon in the peroxidative reactions at low concentrations. Figure 4 shows the peroxidation of TBPD by CPO. These observations indicate that the peroxidation reaction can be catalyzed without the substrate molecule or its reactive moiety having access to the heme center or edge of the buried active site of CPO. It is to be noted that ABTS is also a molecule that exceeds the linear dimension of CPO's active site (*14, 28*). Nanomolar levels of CPO converted this substrate at rates of $\sim 10^3$ per second at acidic pH, rivaling the activity of the celebrated peroxidase from horseradish roots.

4. Utilization of Peroxides in CPO-Catalyzed Peroxidations. Earlier studies have shown that in active-site epoxi-

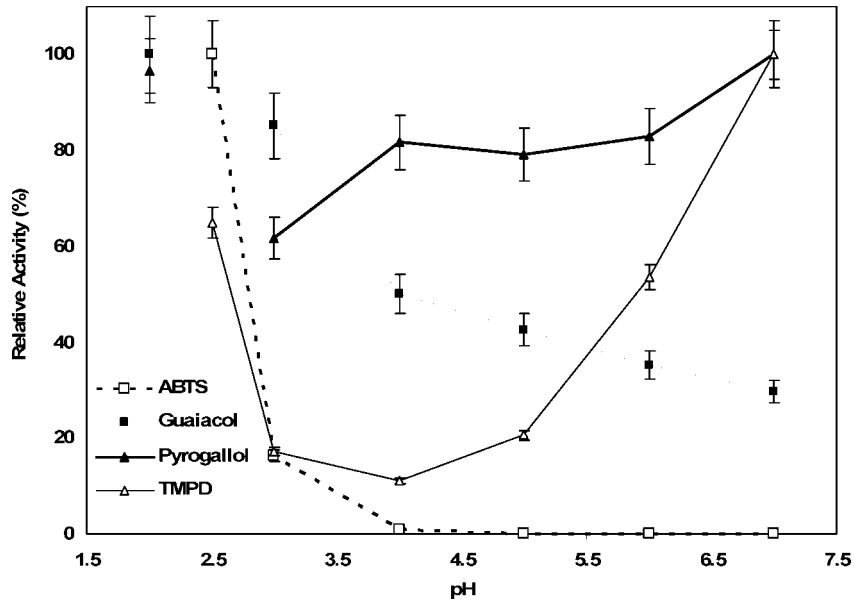

FIGURE 2: Effect of pH on initial rates of peroxidation of various substrates. For ABTS peroxidation, initial concentrations were [ABTS] = 2 mM, [H_2O_2] = 2 mM, and [CPO] = 3 nM. TMPD peroxidation, initial concentrations were [TMPD] = 2 mM, [H_2O_2] = 2.4 mM, [CPO] = 165 nM, and 2% CH_3CN. For phenolics, initial concentration of CPO was 43.5 nM and the peroxidative substrates and hydrogen peroxide concentrations were 2 mM. Rate is given in units of nanomolar substrate converted by nanomolar enzyme per second. The activities for different substrates at the optimal pH were 880, 20, 5, and 235 s^{-1}, respectively.

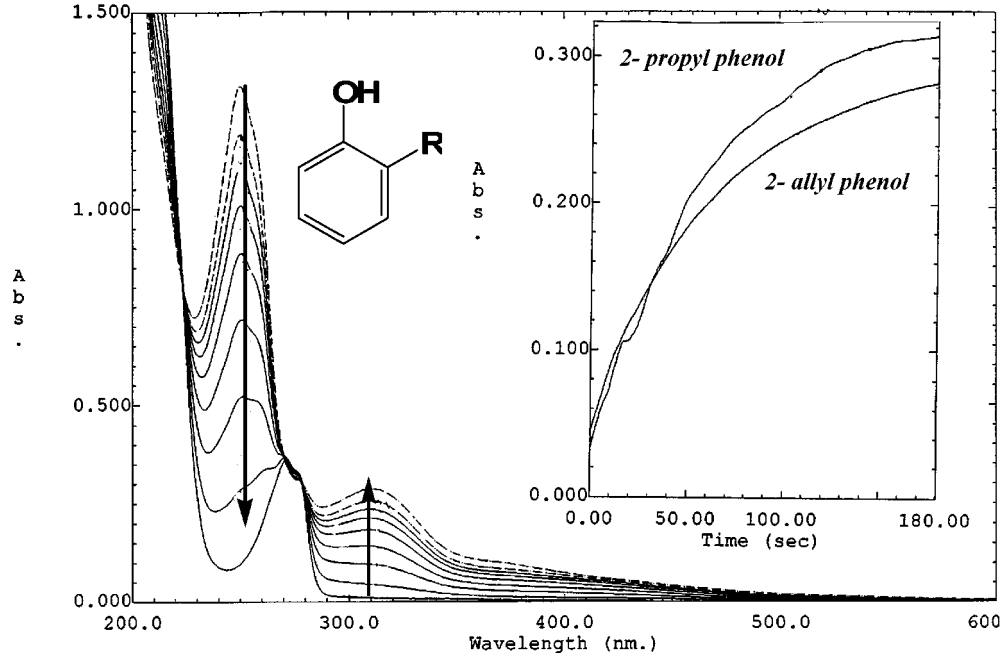

FIGURE 3: Substitution effects on peroxidation of *ortho*-cresols. Initial conditions were cresols at 200 μM, 2 mM EtOOH, 30 nM CPO, pH 4, 313 nm, and 5% CH_3CN. The inset shows the time profiles for the allyl- and propyl-substituted *ortho*-phenolics at 315 nm.

dation and sulfoxidation reactions, hydrogen peroxide serves as a superior activator or oxygen donor compared with alkyl hydroperoxides (*13*). Also, the homosubstrate peroxide dismutation reaction occurs faster with H_2O_2. In the chlorination also, hydrogen peroxide is a more efficient substrate (result not shown). In contrast, ethyl hydroperoxide (EtOOH) served as a much better substrate for TMPD and ABTS peroxidations (Table 2). Under identical conditions, depending upon the substrate type and the concentration of reaction components, the peroxidation rates afforded by EtOOH were anywhere from 10^0 to 10^2 times greater than the rate afforded by H_2O_2. Also, the enzyme showed lower dependence on ABTS concentrations with EtOOH than with hydrogen peroxide. Works from Hollenberg's group had earlier indicated that ethyl hydroperoxide gave high activities in the N-demethylation reactions catalyzed by CPO (*29*).

The rate of peroxide depletion is markedly lowered in peroxidative reactions. For example, in the case of an active site dismutation reaction with 100 nM CPO and 1 mM H_2O_2, peroxide was depleted by more than 98% in less than 2 min. In contrast, more than 50% peroxide remained in the reaction when a peroxidative substrate was present, even after 10 min. Therefore, it was envisaged that addition of a peroxidative substrate could perhaps increase the conversion of the epoxidation substrate, a desired aspect from an applicatory perspective (*13*). On the contrary, it was observed that the

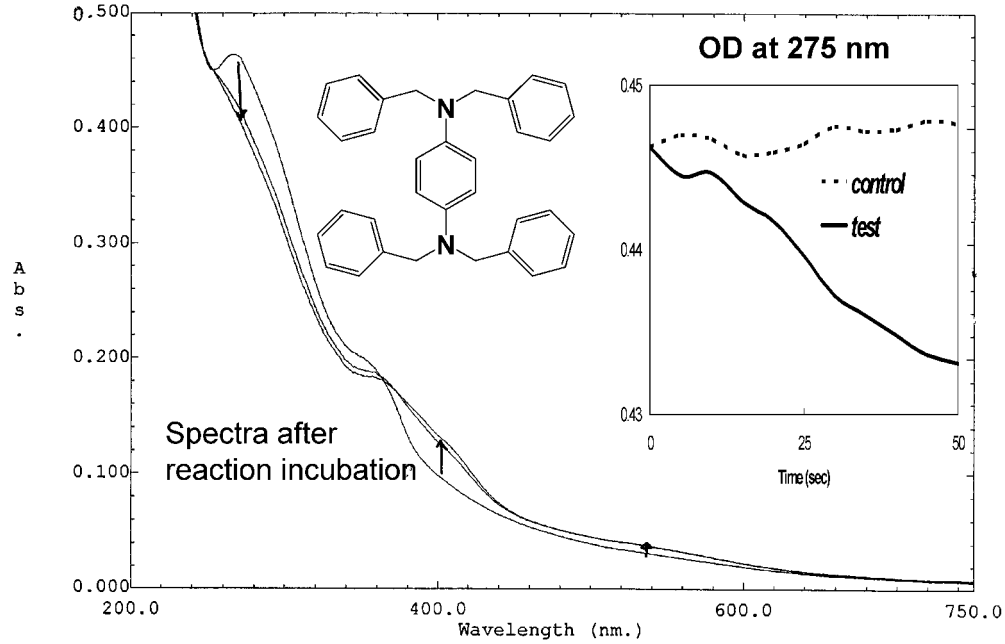

FIGURE 4: Peroxidation of TBPD by CPO. Initial conditions were 2 mM EtOOH, 30 nM CPO, and pH 6.5. Reaction profiles at 400 nm are shown in the inset for a reaction with CH_3CN as cosolvent.

Table 2: Effect of Peroxide and Substrate Concentration on Peroxidation Reactions[a]

	rate				
	TMPD (s^{-1})		ABTS (s^{-1})		
reaction	125 μM	2.5 mM	100 μM	500 μM	1 mM
H_2O_2	0.06	5.61	55.6	314.8	361.1
EtOOH	9.49	61.28	222.2	388.9	527.8

[a] TMPD reactions were carried out at pH 6, 120 nM CPO, and 2.4 mM peroxides, with 2% CH_3CN. ABTS reactions were carried out at pH 3, 3 nM CPO, and 2 mM peroxides. Numerical values given are nanomolar product formed by nanomolar CPO per second.

presence of peroxidative substrates like ABTS and TMPD only lowered the conversion of an epoxidative substrate like styrene (results not shown). This observation implies that the presence of the peroxidative substrates prevented the accumulation of the catalytic intermediate(s) responsible for epoxidation and dismutation reactions.

DISCUSSION

The results presented in Table 1 and Figure 1 clearly show the differential effect of the reaction of dialkyl pyrocarbonate-treated enzyme on CPO reactions. Those reactions that involve binding of substrates at the active heme site are inhibited, while peroxidation reactions are essentially not inhibited. The essential His105 residue is hydrogen bonded to the distal glutamic acid residue (Glu183) (*23, 24*). The latter probably functions as an acid–base catalyst in the formation of CPO's compound I and its subsequent active site reactions. Our results indicate that His105 is not critical for compound I formation in CPO. The lack of inhibition of CPO's peroxidative reactions (upon derivatization with pyrocarbonate) suggests that these reactions predominantly do not occur at the heme active site. Instead, the compound I oxidative equivalents are channeled to surface residues that participate in the peroxidation reactions. This speculation is also furthered by the facts that (1) peroxidative substrates neither show a typical Michaelis–Menten kinetics like epoxidation/dismutation substrates (*13, 21*) nor a zeroth-order kinetics like chlorination reactions (*14*) but exhibit a case that is intermediate, as evident from Table 2 and ref *17*, (2) the presence of more than one optimal pH range for enzyme activity suggests the substrate binding to different amino acid residues, and (3) the presence of peroxidative substrates affords a lower depletion rate of peroxides. Therefore, there are at least two different sites in CPO for carrying out oxidative reactions.

CPO's functional analogues like vanadium peroxidase and horseradish, soybean, and turnip peroxidases show the usual bell-shaped profiles for the peroxidation reaction (*30–33*). CPO also shows relatively conventional pH profiles in peroxide dismutation, oxygen insertion (sulfoxidation and epoxidation), and halogenation reactions (*13, 14*). In contrast, the current study shows that CPO exhibited quite variable pH optima for the peroxidation of different amine substrates. Even in the reaction between CPO and the single substrate of TMPD, two pH optima were observed, separated by four pH units. Most likely, this finding suggests two different mechanisms for the peroxidation reaction. Previous studies reported an acidic pH optimum for chloride-assisted peroxidation reactions and another pH optimum (pH 5) for peroxidations carried out in the absence of chloride ion (*34*). These observations can be explained by the fact that in the presence of chloride ions, a diffusible chlorinating intermediate was being produced and this chlorinating intermediate can carry out peroxidations on its own. All of the peroxidations reported in this study were carried out in the absence of chloride. Hence, the different pH optima (reported in this study) must be based on different reaction sites.

Access to the buried heme in CPO is only available via a relatively narrow channel (*23, 24*). Results from epoxidation experiments indicate that substrates that have greater than 10 linear carbon atoms cannot reach the buried heme (*14, 28*). The efficient peroxidation of ABTS and other large substrates

Scheme 2: A Simple Mechanistic Route for Some Reactions Catalyzed by CPO

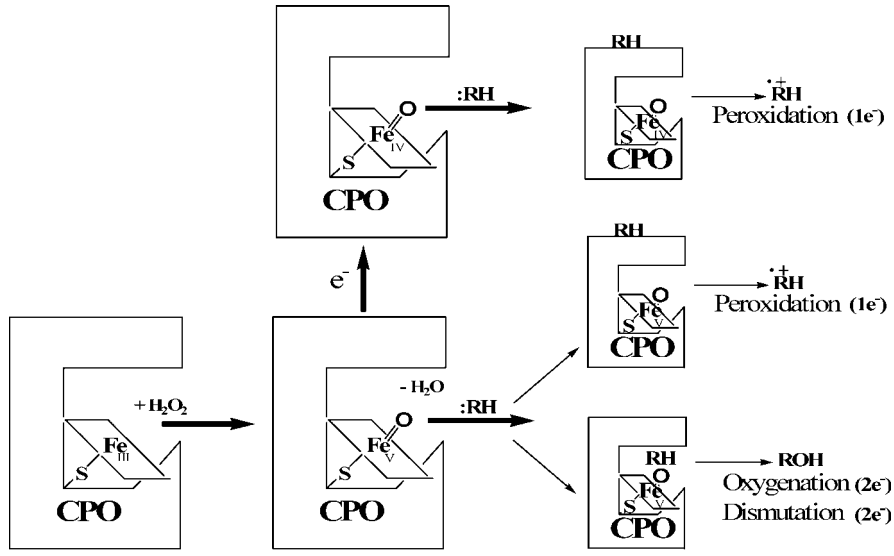

like TBPD supports the conclusion that these peroxidations do not occur at the heme active site of CPO. Surely, a molecule like TBPD cannot access the heme active site and most likely binds to a surface site for its peroxidation reaction.

Most peroxidative substrates show a high reaction rate at low pH perhaps because CPO's redox potential is higher in this environment (*35*). The pH optima for the peroxidation of phenolics shows less variation when compared with the oxidation of amines, and the oxidation rates for phenolics varied over a wide range. The turnover number under optimized conditions for the peroxidation of ABTS is $\sim 10^3$, and it decreases in the series pyrogallol > TMPD > guaiacol. We could rationalize this to be in accordance with the substrates' redox potentials. The catalytic efficiency (k_{cat}/pseudo-K_M) for the CPO-catalyzed peroxidation of ABTS is $\sim 2 \times 10^5$ M^{-1} s^{-1} at pH 3. (Here, a pseudo-K_M is used because the steady-state catalysis profile observed by varying the substrate at fixed enzyme and peroxide concentrations gave atypical kinetics. A linear correlation was obtained with Eadie−Hofstee treatment for only a narrow range of substrate concentrations.) Thus, CPO is as good at peroxidation as horseradish peroxidase, which has a catalytic efficiency of 1.8×10^5 M^{-1} s^{-1} (*36*). Recently, turnip peroxidase (which prefers storage conditions at lower temperatures and which has a catalytic efficiency of only 5×10^2 M^{-1} s^{-1} for ABTS at pH 4.5) has been proposed for peroxidative applications at acidic pH (*33*). The more rugged CPO, with half-life of several days at room temperature, could be used in peroxidative applications at acidic pH ranges, where HRP is relatively inefficient.

In all of CPO's heme active-site oxidations, for example, sulfoxidation, epoxidation, and peroxide dismutations, hydrogen peroxide serves as a superior substrate (*13*). Surprisingly, ethyl hydroperoxide is a superior substrate for peroxidation reactions. Chloroperoxidase has a powerful catalase activity that rapidly dismutates hydrogen peroxide to oxygen and water. The first step in the dismutation reaction is the formation of CPO compound I, and the second step is the reaction of compound I with a second molecule of hydrogen peroxide to form molecular oxygen. It is also surprising that the rate of peroxide depletion is markedly lowered in peroxidative reactions. Perhaps both of the surprises outlined above can be explained by having a lower concentration of compound I. The rate of compound I formation is slower with organic peroxides when compared with the rate with hydrogen peroxide. In the peroxidation reactions, compound I is converted to compound II in the second step, giving a lower transient concentration of compound I.

The heme-thiolate structure and similar magnitudes of kinetic isotope effects for cytochrome P450s and CPO were used to postulate that both the enzymes carry out the heteroatom dealkylation reaction via the same mechanism (*37*). But recently, radical probes have been used to differentiate the mechanistic chemistry (*38*). We could envisage that such a catalytic process of heteroatom dealkylation involving an electron dense heteroatom could potentially be mediated via at least two primary mechanisms, electron or hydrogen atom abstraction (*39*). The crucial point that our work contributes to the ongoing debate is that a sterically hindered substrate could also undergo peroxidative dealkylation without the necessity of going through the oxygen rebound mechanism at the heme center. Since hydrogen tunneling remains a questionable option (*40*), we opine that oxidation of bulky substrates would essentially involve an electron abstraction mechanism.

In summary, chloroperoxidase appears to present different faces to carry out one- and two-electron oxidation reactions. We propose that the two-electron oxidations all involve the active-site reaction of compound I with the oxidation substrate at the distal heme site, while the peroxidation reactions occur predominantly at the surface the enzyme molecule (Scheme 2).

ACKNOWLEDGMENT

The authors acknowledge stimulating discussions with Prof. Alexander Scheeline (UIUC).

REFERENCES

1. Myneni, S. C. (2002) Formation of stable chlorinated hydrocarbons in weathering plant material. *Science 295*, 1039–1041.
2. Casey, W. H. (2002) The fate of chlorine in soils. *Science 295*, 985–986.

3. Shaw, P. D., and Hager, L. P. (1961) Chlorination. VI. Chloroperoxidase: A component of the β-ketoadipate chlorinase system. *J. Biol. Chem. 236*, 1626–1630.
4. Manoj, K. M., and Hager, L. P. (2002) The catalytic utility and versatility of chloroperoxidase. *Recent Res. Dev. Org. Chem. 6*, 392–405.
5. Hager, L. P., Morris, D. R., Brown, F. S., and Eberwein, H. (1966) Chloroperoxidase II: Utilization of halogen ions. *J. Biol. Chem. 241*, 1769–1776.
6. Geigert, J., Niedelman, S. L., and Daleitos, D. J. (1983) Novel haloperoxidase substrates: Alkynes and cyclopropanes. *J. Biol. Chem. 258*, 2273–2277.
7. Griffin, B. W., and Ashley, P. L. (1984) Evidence for a radical mechanism of halogenation of monochlorodimedone catalyzed by chloroperoxidase. *Arch. Biochem. Biophys. 233*, 188–196.
8. Colonna, S., Nagerro, N., Manfredi, A., Castella, L., Gullotti, M., Carrea, G., and Pasta, P. (1990) Enantioselective oxidations of sulfides catalyzed by chloroperoxidase. *Biochemistry 29*, 10465–10468.
9. Allain, E. J., Hager, L. P., Deng, L., and Jacobsen, E. N. (1993) Highly enantioselective epoxidation of disubstituted alkenes with hydrogen peroxide catalyzed by chloroperoxidase. *J. Am. Chem. Soc. 115*, 4415–4416.
10. Zaks, A., and Dodds, D. R. (1995) Chloroperoxidase-catalyzed asymmetric oxidations: substrate specificity and mechanistic study. *J. Am. Chem. Soc. 117*, 10419–10424.
11. Lambier, A. M., Dunford, H. B., and Pickard, M. A. (1987) Kinetics of the oxidation of ascorbic acid ferrocyanide and p-phenolsulfonic acid by chloroperoxidase compounds I and II. *Eur. J. Biochem. 163*, 123–127.
12. Yi, X., Mroczko, M., Manoj, K. M., Wang, X., and Hager, L. P. (1999) Replacement of the proximal heme thiolate ligand with a histidine in chloroperoxidase. *Proc. Natl. Acad. Sci. U.S.A. 96*, 12412–12417.
13. Manoj, K. M., and Hager, L. P. (2001) Utilization of peroxide and its relevance in oxygen insertion reactions catalyzed by chloroperoxidase. *Biochim. Biophys. Acta 1547*, 408–417.
14. Manoj, K. M. (2006) Chlorinations catalyzed by chloroperoxidase occur via a diffusible intermediate and the reaction components play multiple roles in the overall process. *Biochim. Biophys. Acta: Proteins Proteomics 1764*, 1325–1339.
15. Blanke, S. R., Martinis, S. A., Sligar, S. G., Hager, L. P., Rux, J. J., and Dawson, J. H. (1996) Probing the heme coordination structure of alkaline chloroperoxidase. *Biochemistry 35*, 14537–14543.
16. Childs, R. E., and Bardsley, W. G. (1975) The steady-state kinetics of peroxidase with 2,2′-azino-di-(3 ethyl-benzthiazoline-6-sulphonic acid) as chromogen. *Biochem. J. 145*, 93–103.
17. Sun, W., Kadima, T. A., Pickard, M. A., and Dunford, B. H. (1994) Catalase activity of chloroperoxidase and its interaction with peroxidase activity. *Biochem. Cell Biol. 72*, 321–331.
18. Sigma (1995) http://www.sigmaaldrich.com/img/assets/18240/Peroxidase,_Insoluble.pdf.
19. Maehly, A. C., and Chance, B. (1954) Assay of catalases and peroxidases. *Methods Biochem. Anal. 1*, 357–424.
20. Doerge, D. R., Divi, R. L., and Churchwell, M. I. (1997) Identification of colored guaiacol oxidation product produced by peroxidases. *Anal. Biochem. 250*, 10–17.
21. Manoj, K. M., Yi, X., Rai, G. P., and Hager, L. P. (1999) A kinetic epoxidation assay for chloroperoxidase. *Biochem. Biophys. Res. Commun. 206*, 301–303.
22. Blanke, S. R., and Hager, L. P. (1990) Chemical modification of chloroperoxidase with diethylpyrocarbonate: Evidence for the presence of an essential histidine residue. *J. Biol. Chem. 265*, 12454–12461.
23. Sundaramoorthy, M., Terner, J., and Poulos, T. L. (1995) The crystal structure of chloroperoxidase: A heme peroxidase-cytochrome P450 functional hybrid. *Structure 3*, 1367–1377.
24. Sundaramoorthy, M., Terner, J., and Poulos, T. L. (1998) Stereochemistry of chloroperoxidase active site: Crystallographic and molecular modelling studies. *Chem. Biol. 5*, 461–473.
25. Samokysczyn, V. M., and Ortiz de Montellano, P. R. (1991) Topology of chloroperoxidase active site: Regiospecificity of heme modification by phenylhydrazine and sodium azide. *Biochemistry 30*, 11646–11653.
26. Casella, L., Poli, S., Gullotti, M., Selvaggini, C., Beringhelli, T., and Marchesini, A. (1994) The chloroperoxidase-catalyzed oxidation of phenols: Mechanism selectivity and characterization of enzyme-substrate complexes. *Biochemistry 33*, 6377–6386.
27. Dexter, A. F., and Hager, L. P. (1995) Transient heme N-alkylation of chloroperoxidase by terminal alkenes and alkynes. *J. Am. Chem. Soc. 117*, 817–818.
28. Lakner, F. J., and Hager, L. P. (1996) Enantioselective epoxidation of ω-bromo-2-methyl-1-alkenes catalyzed by chloroperoxidase: Effect of chain length on selectivity and efficiency. *J. Am. Chem. Soc. 119*, 443–444.
29. Kedderis, G. L., Koop, D. R., and Hollenberg, P. F. (1980) N-Demthylation reactions catalyzed by chloroperoxidase. *J. Biol. Chem. 255*, 10174–10182.
30. ten Brink, H. B., Dekker, H. L., Schoemaker, H. E., and Wever, R. (2000) Oxidation reactions catalyzed by vanadium chloroperoxidase from curvularia inaequalis. *J. Inorg. Biochem. 80*, 91–98.
31. Kedderis, G. L., and Hollenberg, P. F. (1983) Characterization of the N-demethylation reactions catalyzed by horseradish peroxidase. *J. Biol. Chem. 258*, 8129–8138.
32. Kamal, J. K. A., and Behere, D. V. (2003) Activity, stability and conformational flexibility of seedcoat soyabean peroxidase. *J. Inorg. Biochem. 94*, 236–242.
33. Duarte-Vazquez, M. A., Garcia-Almendarez, B. E., Regalado, C., and Whitaker, J. R. (2001) Purification and properties of a neutral peroxidase isozyme from turnip (*Brassica napus* L. Var. Purple Top White Globe) roots. *J. Agric. Food Chem. 49*, 4450–4456.
34. Thomas, J. A., Morris, D. R., and Hager, L. P. (1970) Chloroperoxidase VII: Classical peroxidatic, catalatic and halogenating forms of the enzyme. *J. Biol. Chem. 245*, 3129–3134.
35. Makino, R., Chiang, R., and Hager, L. P. (1976) Oxidation−reduction potential measurements on chloroperoxidase and its complexes. *Biochemistry 15*, 4748–4754.
36. Nagy, J. M., Kass, A. E. G., and Brown, K. A. (1997) Purification and characterization of recombinant catalase-peroxidase, which confers isoniazid sensitivity in *Mycobacterium tuberculosis*. *J. Biol. Chem. 272*, 31265–31271.
37. Hollenberg, P. F. (1992) Mechanisms of cytochrome P450 and peroxidase catalyzed xenobiotic metabolism. *FASEB J. 6*, 686–694.
38. Bhakta, M. N., and Wimalasena, K. (2005) A mechanistic comparison between cytochrome P450 and chloroperoxidase catalyzed N-dealkylation of *N*,*N*-dialkyl anilines. *Eur. J. Org. Chem. 22*, 4801–4805.
39. Okazaki, O., and Guegerich, F. P. (1993) Evidence for specific base catalysis in N-dealkylation reactions catalyzed by cytochrome P450 and chloroperoxidase: Differences in rates of deprotonation of aminium radicals as an explanation for high kinetic isotope effects observed with peroxidases. *J. Biol. Chem. 268*, 1546–1552.
40. Doll, K. M., Bender, B. R., and Finke, R. G. (2003) The first experimental test of the hypothesis that enzymes have evolved to enhance hydrogen tunneling. *J. Am. Chem. Soc. 125*, 10877–10884.

BI7022656